

# Injection seeded single mode intra-cavity absorption spectroscopy

B. Scherer · W. Salzmann · J. Wöllenstein ·  
M. Weidemüller

Received: 17 December 2008 / Revised version: 26 February 2009 / Published online: 2 April 2009  
© Springer-Verlag 2009

**Abstract** We present a single mode intra-cavity spectroscopy system in which the test laser is locked to a narrow band external single mode laser. This technique solves many problems typically encountered in single mode intra-cavity spectroscopy: it results in good tuning properties, a stable single mode operation close to the lasing threshold, a high side-mode suppression and a reduction of spontaneous emission without the use of any frequency selective element. Measurements of broadband absorptions as well as measurements of a narrow band absorption line of the oxygen A-band are presented and compared with theoretical model predictions. The prototype described in this work provides an enhancement in sensitivity of approximately a factor of 12, and it demonstrates the influence of optical injection to single mode intra-cavity spectroscopy. As there is no need for any frequency selective element inside the cavity, the sensitivity can be massively enhanced by optimizing the laser cavity.

**PACS** 42.62.Fi · 42.55.Px · 07.07.Df

## 1 Introduction

For absolute concentration measurements of trace gases different methods are used to enlarge the sensitivity of conventional absorption spectroscopy [1]. Spectroscopic methods like cavity ring-down spectroscopy (CRDS) or cavity enhanced absorption spectroscopy (CEAS) [2] are based on multipass absorption and provide high sensitivities in terms of an enlargement of the optical pathlength for a given measurement volume. Multimode intra-cavity absorption spectroscopy (ICAS) [3] is one of the most sensitive absorption spectroscopy techniques and utilizes the strong sensitivity of the emission spectra of broadband multimode lasers to narrow band absorptions inside the laser cavity. This method is therefore based on changes in mode dynamics and mode competition due to spectrally selective extinctions inside the laser cavity. Extensive reviews of CRDS and multimode ICAS can be found in [1–6], and a comparative analysis of both methods was performed in [7].

ICAS using a single mode laser is not so sensitive and has not received much attention in the literature [8, 9]. However, in contrast to multimode ICAS, its spectral resolution is only limited by the linewidth of the laser, and in principle no spectral analysis of the output signal is needed. This technical advantage makes single mode ICAS very suitable as a compact and mobile measurement system with high spectral resolution.

The emission of single mode lasers close to the laser threshold is highly sensitive to additional losses inside the cavity. Thus a sensitive and quantitative absorption measurement can be made on a test gas or liquid placed inside

---

B. Scherer (✉) · J. Wöllenstein  
Fraunhofer Institute for Physical Measurement Techniques,  
Heidenhofstrasse 8, 79110 Freiburg, Germany  
e-mail: [benjamin.scherer@ipm.fraunhofer.de](mailto:benjamin.scherer@ipm.fraunhofer.de)

W. Salzmann · M. Weidemüller  
Physics Institute, Albert-Ludwigs University Freiburg,  
79104 Freiburg, Germany

*Present address:*  
W. Salzmann  
Fraunhofer Institute for Physical Measurement Techniques,  
Heidenhofstrasse 8, 79110 Freiburg, Germany

*Present address:*  
M. Weidemüller  
Physics Institute, Ruprecht-Karl University Heidelberg,  
69120 Heidelberg, Germany

the laser cavity. The sensitivity of a single mode ICAS system strongly depends on the absorption cross section, the loss rate of the laser, the spontaneous emission of the lasing medium and the pump rate. The sensitivity, in principle, is ultimately limited by spontaneous emission [8] and the highest sensitivity is achieved with lowest laser losses. The maximum sensitivity is achieved at pump rates very close to the laser threshold. At higher pump rates the additional absorption loss can be compensated by additional gain, and the reduction of the output power is insignificant [10]. Therefore, the laser has to be operated at a well-defined pump rate very close to threshold and in addition has to be tunable in wavelength. To avoid mode hops caused by the additional narrow band loss, a high side-mode suppression is necessary even at pump rates very close to threshold. These different requirements are very difficult to combine; e.g., frequency selective elements would increase the losses of the laser cavity and thus reduce the sensitivity.

In this article we present an approach which extends the high resolution single mode ICAS to have good tuning properties. This is achieved by injection locking the test cavity to an external narrow band master laser. This technique satisfies the requirements listed above as it provides a reduction of the spontaneous emission, the option of using a high finesse cavity, and a stable single mode oscillation at low pump rates without the use of any frequency selective elements.

The setup of the injection seeded intra-cavity spectroscopy system is depicted in Fig. 1. The test laser consists of a GaAlAs-diode on a c-mount and an external output coupler at a distance of 15 cm. The rear side of the diode is high reflection coated ( $R_r \approx 94\%$ ), and the front side anti reflection coated ( $R_f \approx 10^{-5}$ ). The laser cavity is formed by the rear side of the diode and the output coupler, which has a reflectivity of 10%. An absorption cell containing the gas under investigation is placed between the diode and the output coupler. The length of the slave laser cavity can be scanned by a piezo element moving the output coupler. For single mode operation, wavelength tunability, high side-mode suppression and reduction of spontaneous emission, the test laser is injection locked to an external narrow band master laser. The master laser is a grating-stabilized external cavity diode laser in Littrow configuration [11] operating at 760 nm wavelength and has a single mode tuning range of 40 GHz. For efficient locking, the output beam of the master laser is mode matched to the test cavity by a lens-pinhole spatial filter and a telescope. Feedback into the master laser caused by reflections from the test cavity is prevented by an optical isolator. Wavelength tuning of the test laser is achieved by tuning the master laser frequency and the cavity length of the slave laser synchronously. Tuning behavior, single mode operation and locking condition of the slave laser can be monitored by an external Fabry-Perot interferometer.

The signal of interest is the laser power with and without additional intra-cavity absorption losses, from which the relative absorption can be determined. For an injection locked diode laser with additional intra-cavity absorption losses  $\gamma_A$ , the number of photons  $M$  in the lasing mode and the inversion of the medium  $N$  can be expressed in terms of a rate equation model [10, 13]:

$$\frac{d}{dt}M = -(\gamma_C + \gamma_A)M + BN_t \left( \frac{N}{N_t} - 1 \right) (M + \sigma) + k_c \sqrt{M_{\text{inj}}/M} M, \quad (1)$$

$$\frac{d}{dt}N = P - N/\tau - BN_t \left( \frac{N}{N_t} - 1 \right) M.$$

Here,  $\gamma_C$  is the broad-band cavity loss rate,  $B$  is the laser gain,  $P$  is the pump rate,  $N_t$  the transparency excitation,  $\tau$  is the decay time of the upper laser level,  $\sigma$  is the ratio of the spontaneous emission rate to the gain per photon and  $k_c = c/2L$  is the coefficient which takes into account the coupling strength of the external injected photon number  $M_{\text{inj}}$  to the test laser cavity. Detailed descriptions of these parameters can be found in [10, 13].

The sensitivity to intra-cavity absorption is often described in the literature [3, 10] in terms of an effective optical pathlength, which is required to obtain the same absorption strength with a conventional single path absorption measurement outside the laser cavity. This effective optical pathlength is defined by the Beer-Lambert absorption law,  $M_{(\gamma_C + \gamma_A)}/M_{(\gamma_C)} = \exp[(\gamma_A/c)L_{\text{eff}}]$ , resulting in [3, 10]:

$$L_{\text{eff}} = \frac{c}{\gamma_A} \ln \left[ \frac{M_{(\gamma_C)} + A}{M_{(\gamma_C + \gamma_A)} + A} \right]. \quad (2)$$

$M_{(\gamma_C + \gamma_A)}$  and  $M_{(\gamma_C)}$  is the photon number with and without additional intra-cavity loss respectively as calculated from (1). We have included an additional term,  $A$ , in (2) to account for the total number of spontaneously emitted photons in modes other than the lasing mode, which are, under experimental conditions, also detected by the photodiode. The total number of spontaneous emitted photons  $A$  is proportional to the inversion  $N$  and contains a dihedral angle factor.

For single mode ICAS in principle, the effective optical pathlength  $L_{\text{eff}}$  depends via  $M_{(\gamma_C + \gamma_A)}$  on the absorption strength of the intra-cavity absorber and becomes larger as the additional intra-cavity absorption becomes lower [10]. This nonlinear behavior of the effective absorption pathlength has to be considered for the calibration of a single mode intra-cavity spectroscopy system.

An alternative definition of the sensitivity can be given by normalizing the effective absorption pathlength to the real length of the absorber:

$$\xi = L_{\text{eff}}/L. \quad (3)$$

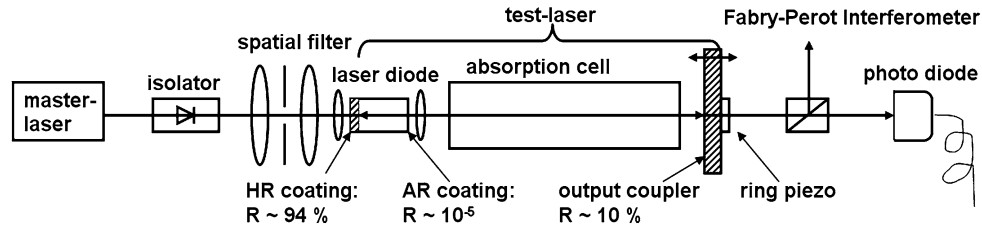


**Fig. 1** Experimental setup of the injection seeded intra-cavity absorption spectrometer. The master laser passes an optical isolator and a lens-pinhole spatial filter to achieve a proper mode coupling to the test laser cavity, which is built by the HR-coated rear side of the test laser

diode and an external output coupler, which is mounted on a ring piezo. The absorber of interest is placed inside the test laser cavity. The output beam is detected by a photo diode and a Fabry-Perot interferometer

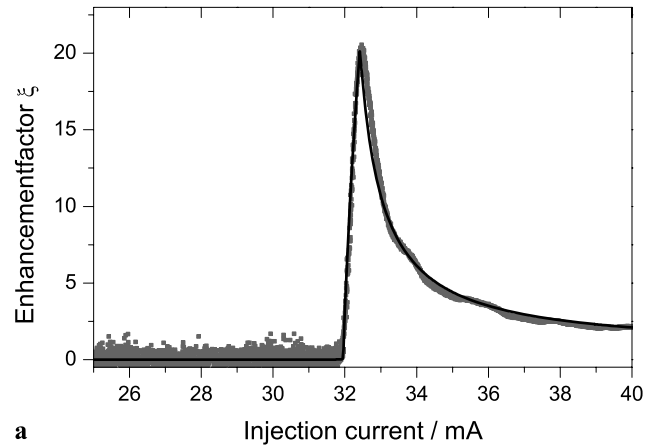
This ratio, known in the literature as the sensitivity enhancement factor [3, 10], describes the sensitivity enhancement of laser intra-cavity absorption compared with the placement of the absorber outside the cavity.  $\xi$  can be determined experimentally by measuring the laser output with and without the intra-cavity absorber and using (2).

For estimating the sensitivity via the rate equations, we used typical laser parameters for a GaAlAs-diode as determined in [10] ( $\tau \approx 10^{-9}$  s,  $N_i \approx 1.5 \times 10^8$ ,  $\sigma \approx 1.6$ ). The gain for the laser used in this work was determined with the procedure described in [10] to be  $B \approx 12(1)$  s $^{-1}$  and the laser losses to be  $\gamma \approx 3.3(5) \times 10^9$  s $^{-1}$ . The unknown spontaneous emission term  $A$  was set as a free parameter.

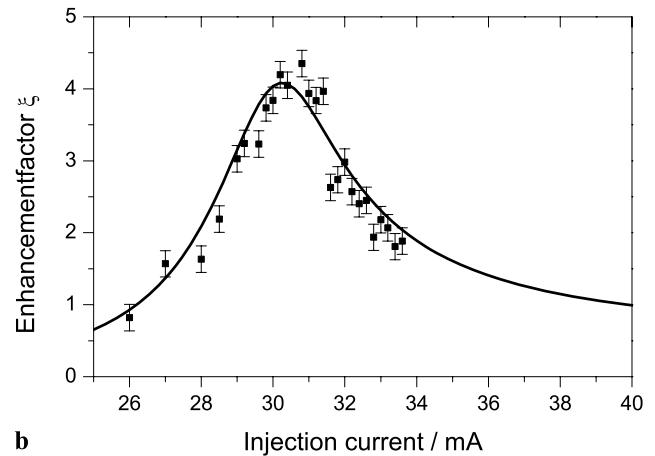
## 2 Broad-band absorption

We first determined the properties of the unseeded system by placing a neutral density filter with 3.7% absorption inside the test laser cavity. The dependence of the enhancement factor  $\xi$  on the laser injection current is shown in Fig. 2(a). The resulting curve (grey line) peaks at a current of 32.6 mA, demonstrating the sensitivity increase close to threshold. Here an enhancement in sensitivity of 21 was achieved. The theoretical sensitivity enhancement, also shown in Fig. 2(a) (black line), was obtained by solving the rate equations (1) using the above parameters and using (2) and (3). The best agreement with the experimental data was obtained when the spontaneously emitted photon number,  $A$ , in modes other than the lasing mode was assumed to be twice as large as the photon number in the lasing mode, which is expected due to the operation close to lasing threshold. The sensitivity profile shows an asymmetric behavior around the maximum which is caused by the strong spontaneous emission in these other modes (parameter  $A$  in (2)).

The resulting sensitivity curve for the injection seeded test laser is shown in Fig. 2(b). As variations of the injection current cause small changes in the cavity length of the test laser, the frequency of the injected light had to be carefully adjusted to the slightly changed resonance frequency after each variation of the injection current. Therefore, in contrast



**a**



**b**

**Fig. 2** Measured (grey) and calculated (black) enhancement factor corresponding to a broad-band absorption of 3.7% without optical injection (a). Measured (dots) and calculated (line) enhancement factor corresponding to a broad-band absorption of 3.7% and an injected optical power of 11.6  $\mu$ W plotted versus injection current (b)

to the unseeded laser, the injection current could not be continuously scanned.

An enhancement in sensitivity of  $\xi \approx 4.6$  could be reached at an injection current of 30.8 mA, slightly lower than the intrinsic threshold without optical injection of 32 mA. The sensitivity enhancement profile of the injection locked laser is more symmetric around the maximum, indi-

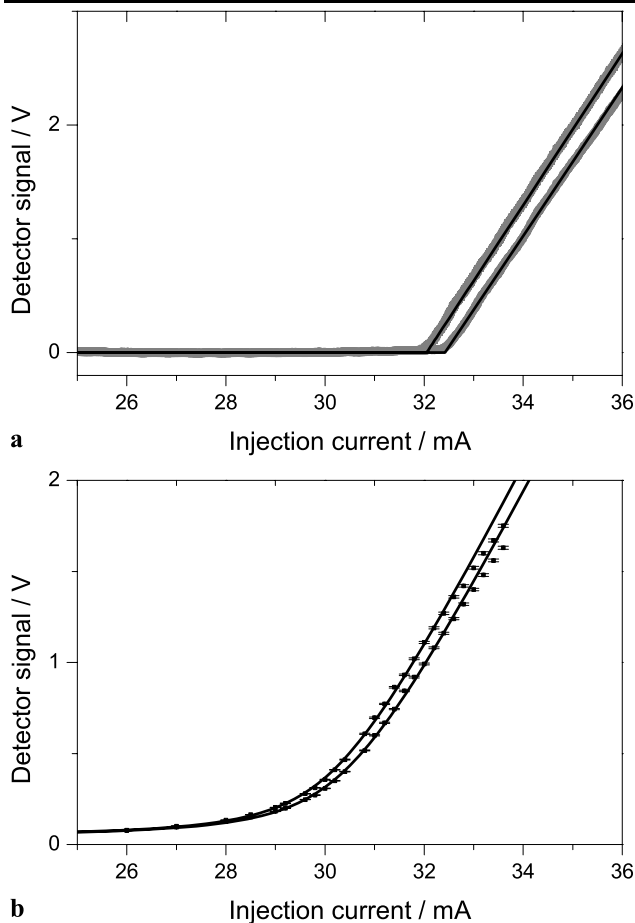


**Fig. 3** Measured (grey) and calculated (black) current-power characteristic with and without additional intra-cavity absorption of 3.7% for the free-running laser (a) and with an injected optical power of 11.6  $\mu\text{W}$  (b)

cating a strong reduction of spontaneous emission compared to the unseeded laser. Indeed, for the calculated sensitivity enhancement (Fig. 2(b) line) the best agreement with the data was obtained by setting the spontaneous emission term  $A$  in modes other than the lasing mode to  $A \approx 0.1M$ , so that the ratio of the spontaneous emission and the photon number in the lasing mode is reduced by 95% compared to the unseeded laser.

Optical injection causes a reduction of the excitation number  $N$ , particularly at very low pump rates below the intrinsic threshold [12, 13], which affects the laser parameters depending on the excitation number  $N$ . In addition, the linear approximation for the total gain  $W \approx B(N - N_t)$  does not hold for very low excitation numbers because of the different saturation behavior in the valence and conduction band [10]. To fit the calculation to the experimental data, the laser gain  $B$  and the transparency excitation  $N_t$  were adjusted to  $B = 14 \text{ s}^{-1}$  and  $N_t = 1.8 \times 10^8$  as compared with the unseeded values  $B = 12 \text{ s}^{-1}$ ,  $N_t = 1.5 \times 10^8$ . This results in a change of the total gain from  $B(N - N_t) =$

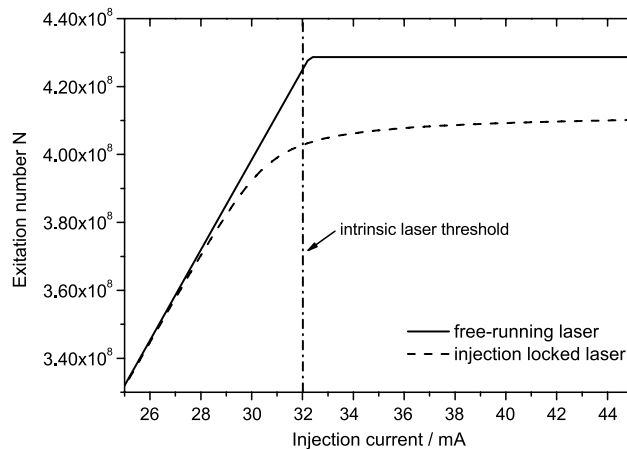


**Fig. 4** Calculated excitation number  $N$  vs. injection current for the free-running laser (solid) and the injection locked laser with  $P_{\text{inj}} = 12 \mu\text{W}$  (dashed). The excitation number  $N$  of the injection locked laser saturates more slowly and the saturation value is reduced compared to the free-running laser. The linear approximation of the total gain  $W \approx B(N - N_t)$  is valid for injection currents above threshold, at which the excitation number is saturated

$3.1 \times 10^9 \text{ s}^{-1}$  in the unseeded case to  $B(N - N_t) = 2.9 \times 10^9 \text{ s}^{-1}$  in the injection seeded case at an injection current of 30.8 mA and corresponds to a reduction of the total gain by 6% due to optically injecting 11.6  $\mu\text{W}$  of laser light. As can be seen in Fig. 3(b), the current-power characteristic of the injection seeded laser is well described by the rate equations using these slightly changed parameters when the injection current is below the intrinsic threshold. However, for injection currents above the intrinsic threshold there are larger deviations between the model and the data due to the non-linearity of the total laser gain  $W$  of an injection seeded laser below its intrinsic laser threshold.

Figure 4 shows the calculated excitation number for the free-running laser (solid line) and the injection locked laser with  $P_{\text{inj}} = 12 \mu\text{W}$  (dashed line) vs. the injection current. The excitation number of the injection locked laser saturates more slowly and the saturated value is lower than that of the free-running laser, which is consistent with the results in [12, 13]. The sensitivity enhancement curve of the injection locked laser peaks at an injection current of 30.8 mA where the excitation number  $N$  is not saturated and the total laser gain  $W$  is not linear in the excitation number  $N$  [10]. Therefore, the rate equation model using these slightly changed parameters is very simplified and only valid for a finite range of pump rates.

Optical injection causes a broadening of the sensitivity profile and a reduction of the maximum reachable sensitivity with increasing injected optical power (Fig. 5). This reduction in sensitivity can be explained by the smoothed laser threshold of the injection seeded laser compared to the unseeded laser (Fig. 3), which lowers the difference of the output power with and without the additional intra-cavity

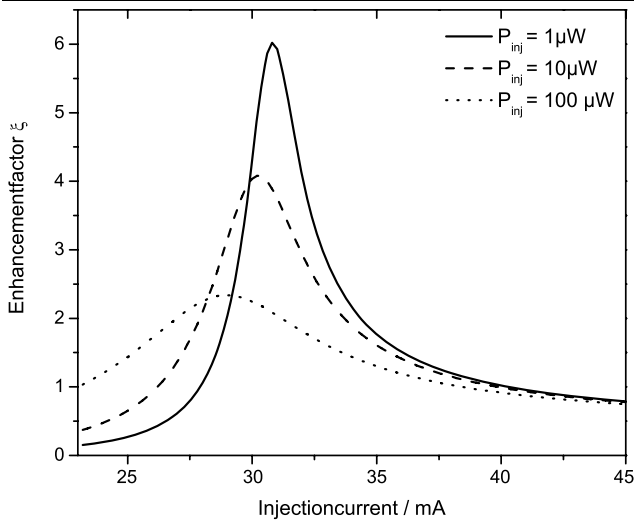


**Fig. 5** Calculated sensitivity enhancement factor vs. injection current for different values of injected optical power. With increasing injected optical power the maximum sensitivity decreases, the sensitivity profile becomes broader and the maximum sensitivity is shifted to lower injection currents

absorber. In addition, optical injection reduces the threshold change due to an additional intra-cavity absorption. The threshold reduction caused by the injected optical power is proportional to  $\sqrt{M/M_{inj}}$  [14]. An additional intra-cavity absorption loss lowers the photon number  $M$  of the free-running laser and increases the threshold reduction due to optical injection. As a consequence, the resulting threshold change caused by an additional intra-cavity absorption loss is reduced by the injected optical power (Fig. 3), which affects the sensitivity in a negative way. To achieve the maximum sensitivity, the injected optical power has to be scaled down to its minimal value for frequency locking.

### 3 Absorption of an oxygen A-band line

As an application the injection seeded intra-cavity absorption technique was applied to narrow band absorption measurements of oxygen. In Fig. 6 the intra-cavity absorption of the P7Q6 line of the oxygen A-band is shown, measured at ambient air with an optical injection of  $50 \mu\text{W}$  and at an injection current of 29 mA. The accuracy of the measured absorption line shape is limited by the nonlinear dependence of the sensitivity enhancement factor on the absorption strength of the intra-cavity absorber (see Sect. 1). Stable single mode operation even at pump rates below the intrinsic threshold and a tuning range of  $1 \text{ cm}^{-1}$  was observed. Wavelength tuning was achieved by tuning the master frequency and the resonance frequency of the test cavity synchronously. In Fig. 6 (black) the frequency of the injected light was tuned exactly to the resonance frequency of the test cavity. The measured absorption corresponds to

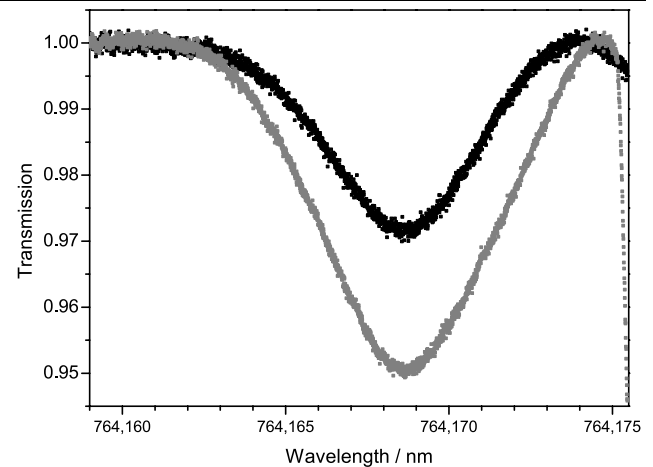


**Fig. 6** P7Q6 line of the oxygen A-band measured in ambient air at an injection current of  $I = 29 \text{ mA}$  and an injected optical power of  $P = 50 \mu\text{W}$ . The master laser frequency and the resonance frequency of the test laser are tuned synchronously without detuning (black curve) and with a detuning of 1 GHz (gray curve). The sudden signal decrease in the latter case at high wavelengths corresponds to a mode-hop of the test laser

an enhancement in sensitivity of  $\xi \approx 6$  consistent with the value found for the broad-band absorber.

The enhancement in sensitivity can be enlarged to  $\xi \approx 12$  by a positive detuning  $\Delta f = f_M - f_T \approx 1 \text{ GHz}$  of the master frequency  $f_M$  from the resonance frequency of the test cavity  $f_T$  within the locking range (Fig. 6 grey), but with negative detuning the sensitivity decreases. As described in [12–14], the decrease of excited carrier density caused by optical injection increases the refractive index in the active medium, which results in a down-shift of the resonance frequency. Optimum locking is achieved when the frequency of the injected light coincides with the resonance frequency of the test laser cavity which is downshifted by optical injection. Therefore, with positive detuning of the injected light from the initial resonance frequency of the test laser cavity the excited carrier number increases, and with negative detuning the carrier density decreases [12–14]. This frequency-dependent change of the total gain caused by optical injection seems to have a strong influence on the sensitivity of ICA measurements.

### 4 Conclusions

In conclusion, we have shown an injection seeded single mode ICAS system which solves most of the typical problems of single mode ICAS. The injection locked intra-cavity laser strongly suppresses spontaneous emission and has a stable single mode oscillation with a strong side-mode suppression, even below its intrinsic threshold. The laser gain can be controlled not only by the injection current but also by the injected optical power and by the frequency of the

injected light. In principle, optical injection lowers the sensitivity of intra-cavity absorption measurements, so the injected optical power has to be reduced to the minimum level for the seeding condition. As there is no need for any frequency selective elements, this disadvantage can be compensated for by optimizing the laser cavity. With a realistically obtainable laser loss rate of  $\gamma \approx 10^7 \text{ s}^{-1}$  ( $R \approx 99\%$ ), we expect an enhancement factor of approximately 500, according to the theoretical model.

Compared to cavity enhanced absorption spectroscopy (CEAS), the method described in this work has a higher sensitivity enhancement for a given mirror reflectivity and is less dependent on the quality factor of the cavity. As the effective steady-state pathlength of a passive cavity is given by  $L_{\text{eff}} = L/(1 - R)$  [2], a CEAS setup with the same mirror reflectivity as used in this work would provide an enhancement in sensitivity of only  $\xi = 1.4$ .

In principle, the setup can be miniaturized and offers the potential for micro-integrated measurement devices.

## References

1. F.K. Tittel, G. Wysocki, A. Kosterev, Y. Bakhrin, *Semiconductor Laser Based Trace Gas Sensor Technology: Recent Advances and Applications, Mid-Infrared Coherent Sources and Applications*. NATO Science Series (Springer, New York, 2008), pp. 467–493
2. B.A. Paldus, A.A. Kachanov, An historical overview of cavity-enhanced methods. *Can. J. Phys.* **83**, 975–999 (2005)
3. V.M. Baev, T. Latz, P.E. Toschek, Laser intracavity absorption spectroscopy. *Appl. Phys. B* **69**, 171 (1999)–202
4. D. Romanini, K.K. Lehmann, Ring-down cavity absorption spectroscopy of the very weak HCN overtone bands with six, seven, and eight stretching quanta. *J. Chem. Phys.* **99**, 6287 (1993)
5. S.E. Vinogradov, A.A. Kachanov, S.A. Kovalenko, E.A. Sviridenkov, Nonlinear dynamics of a multimode dye laser with an adjustable resonator dispersion and implications for the sensitivity of in-resonator laser spectroscopy. *JETP Lett.* **55**, 581 (1992)
6. T. Hänsch, A. Schawlow, P. Toschek, Ultrasensitive response of a CW dye laser to selective extinction. *IEEE J. Quantum. Electron.* **QE-8**, 802 (1972)
7. I. Rahinov, A. Goldman, S. Cheskis, Intracavity laser absorption spectroscopy and cavity ring-down spectroscopy in low-pressure flames. *Appl. Phys. B* **81**, 143 (2005)–149
8. H.J. Kimble, Calculated enhancement for intracavity spectroscopy with a single-mode laser. *IEEE J. Quantum. Electron.* **QE-16**, 455 (1980)
9. W. Gurllit, J.P. Burrows, H. Burkhard, R. Böhm, V.M. Baev, Intracavity diode laser for atmospheric field measurements. *P.E.T. Infrared Phys. Technol.* **37**, 95 (1996)
10. V.M. Baev, J. Eschner, E. Paeth, R. Schüler, P.E. Toschek, Intracavity spectroscopy with diode lasers. *Appl. Phys. B* **55**, 463–477 (1992)
11. L. Ricci, M. Weidemüller, T. Esslinger, A. Hemmerich, C. Zimmermann, V. Vuletic, W. König, T.W. Hänsch, A compact grating-stabilized diode laser system for atomic physics. *Opt. Commun.* **117**, 541–549 (1995)
12. L. Li, A unified description of semiconductor lasers with external light injection and its application to optical bistability. *IEEE J. Quantum Electron.* **30**(8), 1723–1731 (1994)
13. R. Lang, Injection locking properties of a semiconductor laser. *IEEE J. Quantum Electron.* **18**, 976–983 (1982)
14. L. Li, Static and dynamic properties of injection-locked semiconductor lasers. *IEEE J. Quantum Electron.* **30**, 1701–1708 (1994)